Nucleon-pair states of even-even $N = 82$ isotones

Y. Y. Cheng,[1] Y. M. Zhao,[1,2,*] and A. Arima[1,3]

[1]*Department of Physics and Astronomy, Shanghai Jiao Tong University, Shanghai 200240, China*

[2]*IFSA Collaborative Innovation Center, Shanghai Jiao Tong University, Shanghai 200240, China*

[3]*Musashi Gakuen, 1-26-1 Toyotamakami Nerima-ku, Tokyo 176-8533, Japan*

(Received 24 September 2015; revised manuscript received 30 May 2016; published 4 August 2016)

In this paper we study low-lying states of five $N = 82$ isotones, ^{134}Te, ^{136}Xe, ^{138}Ba, ^{140}Ce and ^{142}Nd, within the framework of the nucleon-pair approximation (NPA). For the low-lying yrast states of ^{136}Xe and ^{138}Ba, we calculate the overlaps between the wave functions obtained in the full shell-model (SM) space and those obtained in the truncated NPA space, and find that most of these overlaps are very close to 1. Very interestingly and surprisingly, for most of these yrast states, the SM wave functions are found to be well approximated by one-dimensional, optimized pair basis states, which indicates a simple picture of "nucleon-pair states". The positive-parity yrast states with spin $J > 6$ in these nuclei, as well as the 8_2^+ state, are found to be well described by breaking one or two S pair(s) of the 6_1^+ or 6_2^+ state (low-lying, seniority-two, spin-maximum, and positive-parity); similarly, negative-parity yrast states with spin $J > 9$ are well represented by breaking one or two S pair(s) of the 9_1^- state (low-lying, seniority-two, spin-maximum, and negative-parity). It is shown that the low-lying negative-parity yrast states of ^{136}Xe and ^{138}Ba are reasonably described to be one-octupole-phonon excited states. The evolution of the 6_1^+ and 6_2^+ states for the five isotones are also systematically investigated.

DOI: 10.1103/PhysRevC.94.024307

I. INTRODUCTION

The semimagic $N = 82$ isotones have been of great interest because of the remarkable regularities exhibited in the low-lying states of these nuclei. The long $N = 82$ isotonic chain was studied by using the shell model [1,2] and the quasiparticle random-phase approximation [1,3], in particular, experimental data of energy levels and electromagnetic properties for light even-even $N = 82$ isotones are rich, and have stimulated many shell-model calculations, e.g., Refs. [4–13].

For semimagic nuclei two pair-truncation schemes of the shell model, i.e., the generalized seniority scheme [14–16] and the broken pair approximation [17,18], provide us with appropriate frameworks. Although shell-model calculations for semimagic nuclei are now well within the computer power, the pair-truncation schemes are useful to provide us with a simple picture. Studies of even-even semimagic nuclei within the generalized seniority scheme [19–23] showed that the ground state can be well described by the collective-S-pair condensation, namely seniority-zero state, and a few lowest excited states can be represented by $(N - 1)$ S pairs coupled to two unpaired nucleons (here N is half of the valence nucleon number), namely seniority-two states. Scholten *et al.* studied low-lying states of the light $N = 82$ isotones within the generalized seniority scheme in Ref. [19], where the positive-parity yrast states up to the 6_1^+ state and negative-parity yrast states up to the 9_1^- state were shown to be well described as seniority-two states. In the nucleon-pair approximation, both the seniority-zero and seniority-two states can be represented by one-dimensional pair basis states, as the wave function of one seniority-two state is equivalent to the nucleon-pair basis state constructed by coupling $(N - 1)$ S pairs to one corresponding collective non-S pair. It is therefore interesting to study excited states of the light $N = 82$ isotones with higher spins, in particular to investigate whether the above simple picture of one-dimensional pair configuration survives in these high-spin states.

Octupole correlations between $d_{5/2}$ and $h_{11/2}$ protons and between $g_{7/2}$ and $h_{11/2}$ protons play an important role in low-lying states of the light $N = 82$ isotones. In Ref. [24] $B(E3, 9_1^- \to 6_1^+)$ and $B(E3, 9_1^- \to 6_2^+)$ of ^{134}Te were measured, and an effective charge of valence protons for $B(E3)$ in this region was derived. Recently, the 9_1^- state and the negative-parity level structure above this state in the light even-even $N = 82$ isotones were conjectured to be one-octupole-phonon excited states from corresponding positive-parity states, based on the regularities of experimental energy levels [25,26]. It is interesting to study octupole correlations in the light $N = 82$ isotones, in particular, to microscopically investigate the one-octupole-phonon picture of the negative-parity states.

In this paper we study energy levels, $B(E2)$, $B(E3)$, and magnetic moments of the $N = 82$ isotones ^{134}Te, ^{136}Xe, ^{138}Ba, ^{140}Ce, and ^{142}Nd, within the framework of the nucleon-pair approximation. The paper is organized as follows. In Sec. II we introduce briefly the framework of the nucleon-pair approximation, including the pair basis and the Hamiltonian adopted in this paper. In Sec. III we present and discuss our calculated results of low-lying states for the above five even-even isotones, and in Sec. IV we summarize this paper.

II. THE NUCLEON-PAIR APPROXIMATION OF THE SHELL MODEL

The nucleon-pair approximation (NPA) is an efficient truncation scheme of the shell-model space. If all possible nucleon pairs are considered, the NPA space is equivalent to the full shell-model space; if only a few important pairs are

*Corresponding author: ymzhao@sjtu.edu.cn

considered, the NPA space is much smaller than the exact shell-model space. The general framework of the NPA was proposed in Ref. [27] and refined in Refs. [28,29].

In Ref. [30] the validity of the NPA for semimagic nuclei was studied. In Ref. [31], the electromagnetic properties of the first excited 2^+ states along the semimagic Sn isotopic chain were studied by the SD pair approximation. For a comprehensive review of the NPA formalism and its applications, see Ref. [32].

A. Nucleon-pair basis

In the NPA, the configuration space is constructed by using collective nucleon pairs defined as follows.

$$\begin{aligned} A^{r\dagger}|0\rangle &= \sum_{ab} y(abr)A^{r\dagger}(ab)|0\rangle, \\ A^{r\dagger}(ab) &= (C_a^\dagger \times C_b^\dagger)^r. \end{aligned} \tag{1}$$

Here r is the spin of the collective pair, $C_a^\dagger$ is a creation operator for a nucleon in the a orbit, and $A^{r\dagger}(ab)$ is a creation operator of a noncollective pair with one nucleon in the a orbit and the other in the b orbit. The collective pair with spin r is represented by a linear combination of noncollective pairs with spin r. $y(abr)$ is called structure coefficient. For a system with $2N$ valence nucleons, a basis is constructed by coupling N collective nucleon pairs successively,

$$((A^{r_1\dagger} \times A^{r_2\dagger})^{(J_2)} \times \cdots \times A^{r_N\dagger})^{(J_N)}|0\rangle. \tag{2}$$

In this work, the structure coefficients are obtained in the following procedures. We consider first the collective S pair, denoted by $S^\dagger = \sum_j y(jj0)(C_j^\dagger \times C_j^\dagger)^{(0)} = \sum_j y(jj0)S_j^\dagger$. The structure coefficients $y(jj0)$, with j running over all the single-particle orbits, are determined variationally, to minimize the energy functional $\langle S^N|H|S^N\rangle/\langle S^N|S^N\rangle$ [17]. As for non-S pairs, we diagonalize the Hamiltonian in the seniority-two space, i.e., in the $(S^\dagger)^{(N-1)}A^{r\dagger}(j_1j_2)$ space [$A^{r\dagger}(j_1j_2)$ is the noncollective pair with spin $r \neq 0$] with j_1, j_2 running over all the single-particle orbits. The lowest-state wave function is written in terms of $(S^\dagger)^{(N-1)}\sum_{j_1j_2} c(j_1j_2)A^{r\dagger}(j_1j_2)$, and we assume $y(j_1j_2r) = c(j_1j_2)$. If the second collective pair with the same spin and parity is also considered, the structure coefficients for it correspond to the second-lowest-state wave function.

B. The shell-model Hamiltonian and electromagnetic multipole operator

In this work we adopt the phenomenological Hamiltonian as follows.

$$\begin{aligned} H \;=\; & \sum_j \varepsilon_j \hat{n}_j - G_0\mathcal{P}^{(0)\dagger}\cdot\tilde{\mathcal{P}}^{(0)} - G_2\mathcal{P}^{(2)\dagger}\cdot\tilde{\mathcal{P}}^{(2)} \\ & -\kappa_2 Q^2\cdot Q^2 - \kappa_3 Q^3\cdot Q^3, \end{aligned} \tag{3}$$

where the one-body and two-body parts are both for valence protons. ε_j is the proton single-particle energies, and G_0, G_2, κ_2, and κ_3 are the strength parameters of the monopole pairing, quadrupole pairing, quadrupole-quadrupole, and octupole-octupole interactions between valence protons. The operators in Eq. (3) are defined as below.

$$\begin{aligned} \mathcal{P}^{(0)\dagger} &= \sum_j \frac{\sqrt{2j+1}}{2}(C_j^+ \times C_j^+)^{(0)}, \\ \mathcal{P}^{(2)\dagger} &= \sum_{jj'} q(jj'2)(C_j^+ \times C_{j'}^+)^{(2)}, \\ \tilde{\mathcal{P}}^{(0)} &= -\sum_j \frac{\sqrt{2j+1}}{2}(\tilde{C}_j \times \tilde{C}_j)^{(0)}, \\ \tilde{\mathcal{P}}^{(2)} &= -\sum_{jj'} q(jj'2)(\tilde{C}_j \times \tilde{C}_{j'})^{(2)}, \\ Q^2 &= \sum_{jj'} q(jj'2)(C_j^+ \times \tilde{C}_{j'})^{(2)}, \\ Q^3 &= \sum_{jj'} q(jj'3)(C_j^+ \times \tilde{C}_{j'})^{(3)}, \\ q(jj'\lambda) &= -\frac{1}{\hat{\lambda}}\frac{(j\|r^\lambda Y^\lambda\|j')}{r_0^\lambda}. \end{aligned} \tag{4}$$

Here $\hat{\lambda} = \sqrt{2\lambda+1}$; r_0 is the oscillator parameter, and $r_0^2 = 1.012A^{1/3}$ fm^2 in this work. For the definition of the reduced matrix element, see Eq. (8.4) of Ref. [16].

In this work, valence protons occupy the 50–82 major shell, which includes the positive-parity $g_{7/2}$,$d_{5/2}$,$d_{3/2}$,$s_{1/2}$ and negative-parity $h_{11/2}$ orbits. The single-particle energies are taken from the single-particle states of ^{133}Sb [33] except for $s_{1/2}$. The single-particle energy of $s_{1/2}$ was not measured yet and we adopt the value from Ref. [34]. The strength parameters of the monopole pairing, quadrupole pairing, quadrupole-quadrupole, and octupole-octupole interactions are adjusted to fit the experimental energy levels and electromagnetic properties. In Table I we list these parameters adopted in this work.

For semimagic nuclei with valence protons, the electric multipole operator is as follows.

$$T(EL) = e_\pi Q_\pi^L r_0^L, \tag{5}$$

TABLE I. Hamiltonian parameters (in unit of MeV) adopted in this work. The single-particle energies are taken from Refs. [33,34]. The strength parameters of the monopole pairing, quadrupole pairing, quadrupole-quadrupole, and octupole-octupole interactions are adjusted to fit experimental data of energy levels and electromagnetic properties. For the monopole pairing and quadrupole pairing interactions, $G_0 = 0.180$ MeV and $G_2 = 0.015$ MeV are adopted for all the five isotones.

	$s_{1/2}$	$d_{3/2}$	$d_{5/2}$	$g_{7/2}$	$h_{11/2}$
ε_j	2.990	2.440	0.962	0.000	2.792
	^{134}Te	^{136}Xe	^{138}Ba	^{140}Ce	^{142}Nd
κ_2	0.045	0.045	0.040	0.035	0.035
κ_3	0.012	0.011	0.008	0.004	0.004

where the operator Q^L is defined in Eq. (4). The reduced electric transition probability is given by

$$B(EL) = \frac{1}{2J_i + 1}(\alpha_f J_f \| T(EL) \| \alpha_i J_i)^2. \quad (6)$$

The magnetic dipole operator is as follows.

$$T(M1) = g_{l\pi} L_\pi + g_{s\pi} S_\pi. \quad (7)$$

The magnetic dipole moment is given by the diagonal matrix element of $T(M1)$,

$$\mu = \sqrt{\frac{4\pi}{3}} \langle JM = J | T(M1) | JM = J \rangle. \quad (8)$$

The one-body operators L and S in Eq. (7) are defined as below,

$$L = \sum_{jj'} q_l(jj'1)(C_j^+ \times \tilde{C}_{j'})^{(1)},$$

$$S = \sum_{jj'} q_s(jj'1)(C_j^+ \times \tilde{C}_{j'})^{(1)},$$

$$q_l(jj'1) = \delta_{ll'}(-1)^{l+1/2+j'} \sqrt{\frac{l(l+1)}{3}} \hat{j}\hat{j}'\hat{l} \begin{Bmatrix} j & j' & 1 \\ l' & l & \frac{1}{2} \end{Bmatrix},$$

$$q_s(jj'1) = \delta_{ll'}(-1)^{l+1/2+j} \frac{1}{\sqrt{2}} \hat{j}\hat{j}' \begin{Bmatrix} j & j' & 1 \\ \frac{1}{2} & \frac{1}{2} & l \end{Bmatrix}.$$

III. RESULTS AND DISCUSSION

A. ^{134}Te, ^{136}Xe, and ^{138}Ba

In this paper we perform three sets of calculation for ^{136}Xe and ^{138}Ba, with our focus on yrast states with positive parity or negative parity, including those with high spins. The first set, denoted as "SM," is performed in the full shell-model configuration space, which is realized in the NPA by considering all possible noncollective pairs. The second set, denoted as "NPA," is performed in the truncated nucleon-pair space, by considering only a few collective S and non-S pairs. In the third set, denoted as "pair state," the configuration space of each state is a *one-dimensional*, optimized nucleon-pair basis state which is in the form of Eq. (2), i.e., a simple configuration assuming no mixings with other basis states. Such optimized nucleon-pair basis state is the largest component in the corresponding NPA wave function. For ^{134}Te, the three configuration spaces are the same.

For the low-lying positive-parity states of ^{136}Xe and ^{138}Ba, valence protons predominantly occupy the $g_{7/2}$ and $d_{5/2}$ orbits; for the low-lying negative-parity states, one proton occupies the abnormal-parity $h_{11/2}$ orbit, with the others in the $g_{7/2}$ and $d_{5/2}$ orbits. By considering occupancies of single-particle orbits, we adopt collective positive-parity pairs with spin zero, two, and four, denoted as S, D, and G, as well as two positive-parity spin-six pairs (to describe both the 6_1^+ and 6_2^+ states), denoted as I_1 and I_2. The structure coefficients of the I_1 and I_2 pairs correspond to the wave functions of the first- and second-lowest 6^+ states obtained in the seniority-two space. For negative-parity states, each pair basis is constructed by one negative-parity pair with spin three or nine, denoted as $\mathcal{F}$ or $\mathcal{L}$, coupled with the above positive-parity pairs. As the yrast states with spin$^{\text{parity}}$ $J^P = 1^+, 3^+, 5^+$ and $4^-, 5^-, 6^-, 7^-, 8^-$ are expected to be seniority-two states, the corresponding seniority-two pair basis $|S^{(N-1)} J^P\rangle$ is additionally included for them.

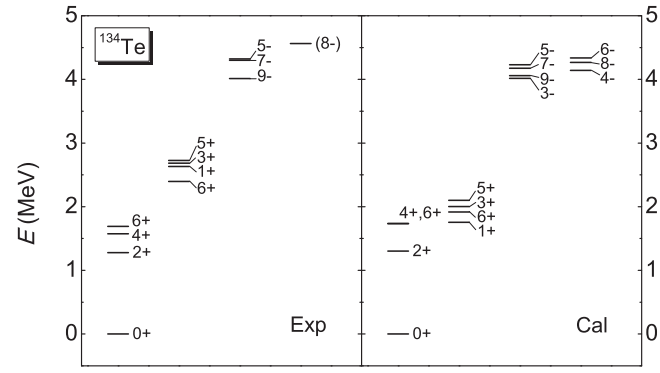

FIG. 1. Calculated energy levels for low-lying states of ^{134}Te, in comparison with experimental data [33].

1. Nucleon-pair states

In Fig. 1 we present the calculated energy levels of the ^{134}Te nucleus, in comparison with experimental data. For the positive-parity states, one sees the experimental energy levels of the 2_1^+, 4_1^+, and 6_1^+ states are well reproduced by calculation, while the calculated energy levels of the 1_1^+, 3_1^+, 5_1^+, and 6_2^+ states are smaller than experimental data. In our calculation, the 2_1^+, 4_1^+, and 6_1^+ states of the ^{134}Te nucleus are dominated by the $|(g_{7/2}g_{7/2}), J\rangle$ configuration, while the 1_1^+, 3_1^+, 5_1^+, and 6_2^+ states are dominated by the $|(g_{7/2}d_{5/2}), J\rangle$ configuration.

In Fig. 2 we present the calculated energy levels of ^{136}Xe and ^{138}Ba obtained in the "SM," "NPA," and "pair state" configuration spaces, respectively, in comparison with experimental data. One sees the experimental energy levels of ^{136}Xe and ^{138}Ba are very well reproduced by the SM calculation with the interaction parameters listed in Table I. One also sees the energy levels obtained in the truncated NPA space are almost the same as those obtained in the full SM space, with very few exceptions. Interestingly, one sees the energy level of each state calculated by using the one-dimensional, optimized pair basis state is also very close to the SM result, with very few exceptions.

In Table II we present calculated $B(E2)$, $B(E3)$ values and magnetic moments (denoted as μ) of ^{134}Te, ^{136}Xe, and ^{138}Ba, and corresponding experimental data. For ^{136}Xe and ^{138}Ba, the results obtained in the three sets of calculations, denoted as "SM," "NPA," and "PS," are presented, respectively. The effective charge of valence protons for $B(E2)$ is set to be $1.7e$, and that for $B(E3)$ is set to be $1.9e$ as suggested in Ref. [24]. $g_{l\pi}$ are optimized to be $1.1\mu_N$, and standard $g_{s\pi} = 5.586 \times 0.7\mu_N$ is adopted in our calculations. In Table II one sees experimental data are well reproduced by the results obtained in the SM space. One also sees most of the results obtained in the truncated NPA space are very close to those obtained in the full SM space, although the $B(E2)$ value is very sensitive to the subtle details of the wave functions, and the μ value

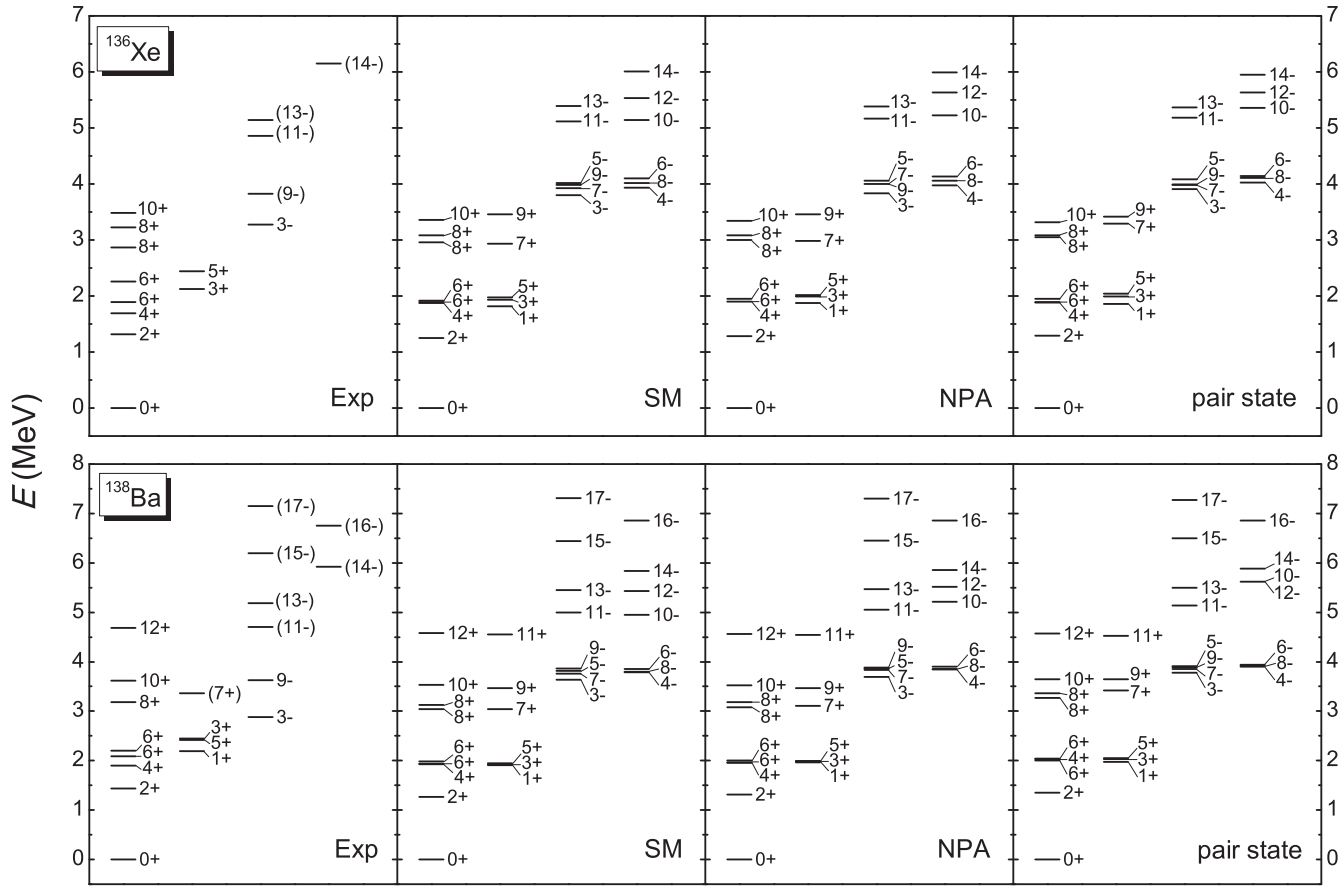

FIG. 2. Energy levels for ^{136}Xe and ^{138}Ba calculated in three configuration spaces, in comparison with experimental data [12,33]. The first space, denoted by "SM," corresponds to the full shell-model configuration space. The second, denoted by "NPA," corresponds to space constructed by using collective pairs with positive parity and spin zero, two, and four, as well as two positive-parity spin-six pairs for positive-parity states, or by coupling the above positive-parity pairs to one negative-parity pair with spin three or nine for negative-parity states. The third, called "pair state," is simply a one-dimensional, optimized nucleon-pair basis state constructed by collective pairs.

is very sensitive to the occupancies of single-j orbits in the wave function. Interestingly, one sees many values given by the optimized pair basis states are in reasonable agreement with the SM results.

Therefore, it is very interesting to compare explicitly the wave functions obtained in the three configuration spaces. In Fig. 3 we present for each yrast state of ^{136}Xe and ^{138}Ba the overlap between the SM wave function and corresponding NPA wave function, the overlap between the NPA wave function and corresponding one-dimensional, optimized nucleon-pair basis state, and the overlap between the SM wave function and the optimized nucleon-pair basis state. One sees the overlaps between the SM wave functions and the NPA wave functions are very close to 1, except for the 12_1^- state of both ^{136}Xe and ^{138}Ba. For the 6_2^+ and 8_2^+ states of ^{136}Xe, the overlaps are 0.97 and 0.98, respectively; and for the two states of ^{138}Ba, the overlaps are 0.99 and 0.96, respectively. These mean the wave functions of these states obtained in the full SM space are well approximated by the wave functions obtained in our truncated NPA space.

One also sees from Fig. 3 that the overlap between the NPA wave function and corresponding optimized nucleon-pair basis state is close to 1, except for the 7_1^+ and 10_1^- states of both ^{136}Xe and ^{138}Ba. This means that for these yrast states the NPA wave function is further reduced to the one-dimensional nucleon-pair basis state at good approximations. Correspondingly, for most yrast states the overlap between the SM wave function and the optimized pair basis state is larger than 0.9. For the 6_2^+ and 8_2^+ states of ^{136}Xe, the overlaps between the SM wave functions and optimized pair basis states are 0.97 and 0.95, respectively; and for the two states of ^{138}Ba, the overlaps are 0.92 and 0.87, respectively. These indicate that for these states of ^{136}Xe and ^{138}Ba, the SM wave function is well represented by the one-dimensional, optimized nucleon-pair basis state. In other words, *one might neglect mixings with other pair basis states as a good approximation*. Therefore we call these states "pair states" to highlight this simple picture.

In Tables III and IV we present the low-lying states of ^{136}Xe and ^{138}Ba in terms of their optimized pair basis states, with the requirement that the overlaps of these pair basis states with corresponding SM wave functions are larger than 0.85. In Tables III and IV, one sees the 0_1^+ states of the two nuclei are seniority-zero states, and the $1_1^+, 2_1^+, 3_1^+, 4_1^+, 5_1^+, 6_1^+, 6_2^+$ states

TABLE II. Calculated $B(E2)$ and $B(E3)$ values (in units of W.u.), and magnetic moments μ (in units of μ_N), as well as experimental data [33] for ^{134}Te, ^{136}Xe, and ^{138}Ba. Notations "SM" and "NPA" are the same as in Fig. 2, and "PS" denotes "pair state" for short. The effective charge of valence protons for $B(E2)$ is $1.7e$, and that for $B(E3)$ is $1.9e$ as assumed in previous study [24]. $g_{l\pi}$ are optimized to be $1.1\mu_N$, and we assume the quenched $g_{s\pi} = 5.586 \times 0.7\mu_N$.

	^{134}Te		^{136}Xe				^{138}Ba			
	Exp	Cal	Exp	SM	NPA	PS	Exp	SM	NPA	PS
$B(E2)$										
$2_1^+ \to 0_1^+$	6.3(20)	5.21	9.68(38)	11.47	10.60	10.23	10.8(5)	14.80	13.49	13.03
$4_1^+ \to 2_1^+$	4.3(4)	4.24	1.281(17)	2.07	0.67	0.56	0.2873(15)	1.77	1.37	0.18
$6_1^+ \to 4_1^+$	2.05(4)	2.41	0.0132(4)	0.33	0.36	0.44	0.053(7)	0.44	0.31	0.06
$6_2^+ \to 4_1^+$	–	0.30	–	0.02	0.07	0.10	–	0.03	0.05	0.01
$8_1^+ \to 6_1^+$	–	–	–	0.17	0.22	0.01	–	8.70	5.50	7.97
$8_1^+ \to 6_2^+$	–	–	–	6.64	5.16	5.38	–	0.72	1.94	<0.01
$8_2^+ \to 6_1^+$	–	–	–	5.40	4.62	5.11	–	0.71	1.85	0.01
$8_2^+ \to 6_2^+$	–	–	–	0.07	0.13	0.01	–	6.46	4.43	8.15
$10_1^+ \to 8_1^+$	–	–	–	6.79	4.51	3.30	1.59(22)	3.18	2.62	0.06
$10_1^+ \to 8_2^+$	–	–	–	0.21	0.47	0.05	–	0.01	0.14	0.20
$12_1^+ \to 10_1^+$	–	–	–	–	–	–	–	0.92	0.60	0.25
$5_1^- \to 3_1^-$	–	4.27	–	2.50	2.42	1.73	–	0.15	0.20	0.35
$7_1^- \to 5_1^-$	–	1.92	–	1.06	1.12	0.76	–	0.89	0.84	0.34
$9_1^- \to 7_1^-$	–	0.15	–	0.01	0.05	0.03	–	0.02	0.03	0.02
$11_1^- \to 9_1^-$	–	–	–	6.16	5.09	5.78	–	10.65	8.75	9.36
$13_1^- \to 11_1^-$	–	–	–	4.65	3.17	2.77	–	0.49	0.09	0.14
$15_1^- \to 13_1^-$	–	–	–	–	–	–	–	5.48	3.67	1.20
$17_1^- \to 15_1^-$	–	–	–	–	–	–	–	0.91	0.27	0.02
$B(E3)$										
$9_1^- \to 6_1^+$	3.80(14)	3.95	–	5.11	2.82	4.61	–	8.23	7.57	11.01
$9_1^- \to 6_2^+$	8.2(3)	9.15	–	6.99	9.03	7.53	–	2.95	3.61	0.32
$11_1^- \to 8_1^+$	–	–	–	9.28	7.82	7.97	–	10.39	10.88	10.01
$11_1^- \to 8_2^+$	–	–	–	3.07	4.04	4.73	–	0.67	0.02	0.37
$13_1^- \to 10_1^+$	–	–	–	9.44	9.76	10.58	–	0.29	1.32	0.55
$15_1^- \to 12_1^+$	–	–	–	–	–	–	–	17.92	18.25	14.94
μ										
2_1^+	–	1.66	1.53(9)	1.95	1.92	1.91	–	2.05	2.03	2.06
4_1^+	–	3.14	3.2(6)	3.21	3.16	3.15	3.2(6)	3.68	3.45	3.53
6_1^+	5.08(15)	5.04	–	5.34	4.98	5.20	5.86(12)	6.07	5.92	6.68
6_2^+	–	6.60	–	6.29	6.64	6.44	–	5.58	5.71	4.96
8_1^+	–	–	–	8.21	8.07	8.34	–	8.46	8.52	8.69
8_2^+	–	–	–	6.94	6.97	7.22	–	7.71	7.42	7.17
10_1^+	–	–	–	10.10	10.10	10.06	–	10.10	10.08	10.12
12_1^+	–	–	–	–	–	–	–	12.83	12.82	12.94

as well as the 3_1^-,4_1^-,5_1^-,6_1^-,7_1^-,8_1^-,9_1^- states are seniority-two states. There are a few pair states which have two or three non-S pairs, such as the 8_1^+, 8_2^+, 10_1^+, 11_1^-, 13_1^- states of both nuclei and the 12_1^+, 15_1^-, 17_1^- states of ^{138}Ba. This indicates that the generalized seniority is a good quantum number here, and that *each of these seniority-four or seniority-six states can be further reduced to a very simple, one-dimensional nucleon-pair basis state with two or three collective non-S pairs.*

In Tables III and IV one sees the 6_1^+ and 6_2^+ states are represented by $|S^{(N-1)}I_1\rangle$ and $|S^{(N-1)}I_2\rangle$ ($N = 2$ for ^{136}Xe and $N = 3$ for ^{138}Ba), respectively. Interestingly, one sees the 8_1^+ and 8_2^+ states are characterized by coupling the D pair to the two positive-parity spin-six pairs, i.e., the I_1 and I_2 pairs, respectively. For ^{136}Xe the 8_1^+ state corresponds to the I_2 pair and the 8_2^+ state corresponds to the I_1 pair, while for ^{138}Ba the 8_1^+ state corresponds to the I_1 pair and the 8_2^+ state corresponds to the I_2 pair.

In addition to the 8_1^+ and 8_2^+ states, the yrast states with positive parity and spin $J > 6$ are represented by the pair basis states having at least one I_1 or I_2 pair, as shown in Tables III and IV. Similarly, the yrast states with negative parity and spin $J > 9$ are represented by the pair states having one $\mathcal{L}$ (i.e., spin-nine and negative-parity) pair. In other words, the low-lying positive-parity yrast states with $J > 6$ are given by breaking one or two S pair(s) of the 6_1^+ or 6_2^+ state (the low-lying, seniority-two, spin-maximum and positive-parity states), and the negative-parity yrast states with $J > 9$ are given by breaking one or two S pair(s) in the 9_1^- state (the low-lying, seniority-two, spin-maximum and negative-parity state); for example, the 9_1^- state of ^{136}Xe is given dominantly by $|S\mathcal{L}\rangle$ and the 11_1^- state by $|D\mathcal{L}\rangle$, and one therefore approximates

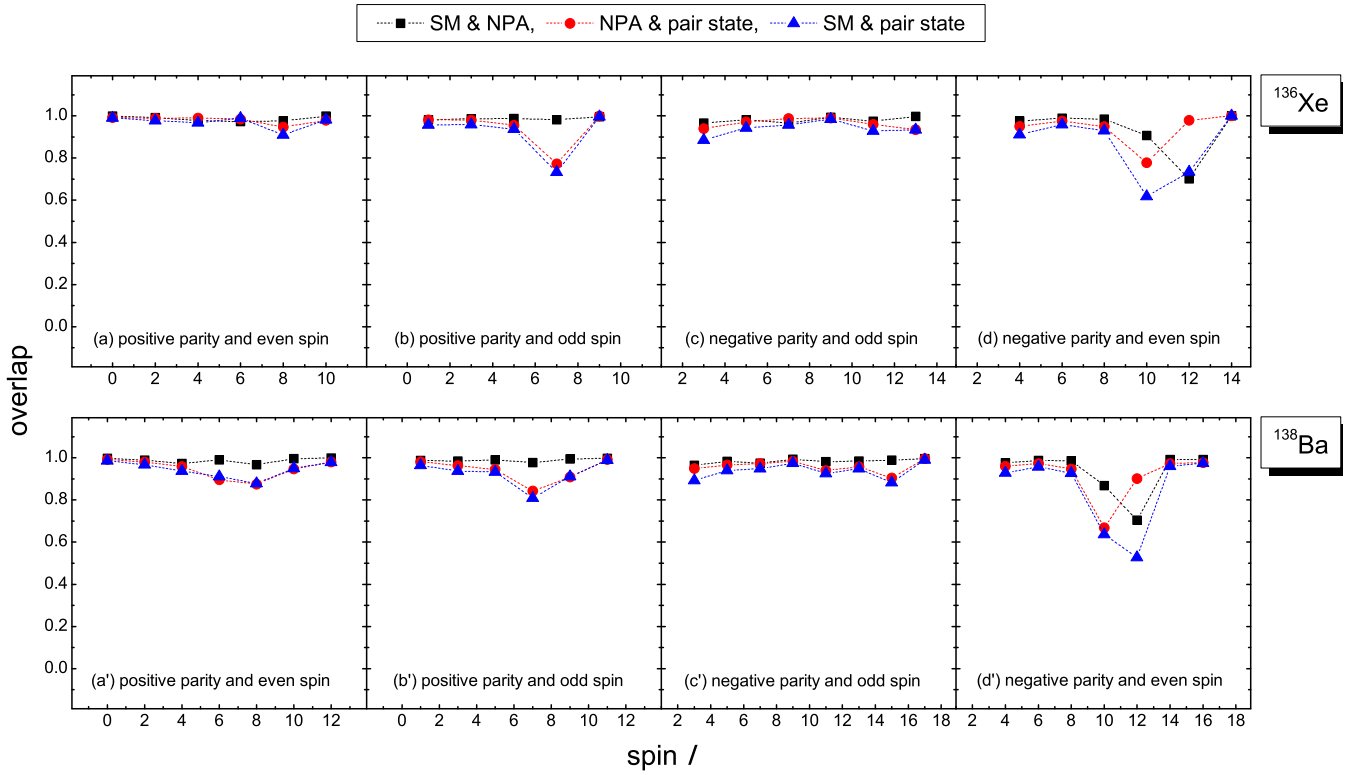

FIG. 3. The overlap between the SM wave function and corresponding NPA wave function (solid black squares), the overlap between the NPA wave function and corresponding one-dimensional, optimized pair basis state (solid red circles), and the overlap between the SM wave function and the optimized pair basis state (solid blue up-triangles), for yrast states of ^{136}Xe and ^{138}Ba. Panels (a) and (a′) [(b) and (b′), (c) and (c′), (d) and (d′)] correspond to the yrast states with positive parity and even spin (positive parity and odd spin, negative parity and odd spin, negative parity and even spin), respectively.

the 11^-_1 state as an excitation of the 9^-_1 state by breaking one S pair into the D pair.

According to Tables III and IV, the 10^+_1 and 14^-_1 states of ^{136}Xe, as well as the 11^+_1, 14^-_1, and 17^-_1 states of ^{138}Ba can be represented optionally by a one-dimensional nucleon-pair basis state; for example, the 17^-_1 state of ^{138}Ba may be well approximated to be either $|r_1 r_2 r_3, J_2\rangle = |G I_1 \mathcal{L}, 10\rangle$, or $|I_1 I_2 \mathcal{L}, 10\rangle$. This is originated from the nonorthogonality of the nucleon-pair basis. In other words, these configurations are very close to each other.

2. *One-octupole-phonon states*

In Refs. [25,26], the one-octupole-phonon picture was suggested for negative-parity states of the light $N = 82$ isotones. The 9^-_1 state and the above negative-parity level structure in ^{136}Xe and ^{138}Ba were conjectured to be formed by coupling one octupole phonon to the positive-parity states. In particular, it was suggested that the 9^-_1 state of ^{136}Xe is given by coupling an octupole phonon to the 6^+_2 state, while the 9^-_1 state of ^{138}Ba is given by coupling an octupole phonon to the 6^+_1 state [25].

We now study the one-octupole-phonon picture for the negative-parity yrast states. We take the Q^3 in the form of Eq. (4) as our octupole phonon operator; we couple this operator to the NPA wave functions of the $6^+_1, 6^+_2, 7^+_1, 8^+_1, 8^+_2, 9^+_1, 10^+_1, 11^+_1, 12^+_1$ states, and normalize the wave functions such obtained, which yields the one-octupole-phonon excited states. We calculate the overlaps between the wave functions of the one-octupole-phonon states and the NPA wave functions of the negative-parity yrast states with spin $J = 9 \sim 15$. Such overlaps are tabulated in Table V, where one sees the octupole-phonon picture explains most of these negative-parity yrast states, except for the 13^-_1 and 14^-_1 states of ^{138}Ba. As shown in Fig. 3, the SM wave functions of the positive-parity and negative-parity states in Table V are well approximated by the NPA wave functions (except for the 12^-_1 state of both nuclei), one therefore expects a similar observation based on the SM wave functions.

In Table V, one also sees that the 9^-_1 state of ^{136}Xe is better represented by coupling the octupole phonon to the 6^+_2 state rather than to the 6^+_1 state, while the 9^-_1 state of ^{138}Ba is better represented by coupling the octupole phonon to the 6^+_1 state. The 11^-_1 state of both nuclei is better represented by coupling the phonon to the 8^+_1 state than to the 8^+_2 state. This is consistent with the dominant configurations of their wave functions shown in Tables III and IV, the 8^+_1 state of ^{136}Xe is given by breaking one S pair of the 6^+_2 state into the D pair, while the 8^+_1 state of ^{138}Ba is given by breaking one S pair of the 6^+_1 state; and the 11^-_1 state of both nuclei is given by breaking one S pair of the 9^+_1 state into the D pair.

B. ^{140}Ce and ^{142}Nd

For ^{140}Ce and ^{142}Nd, we calculate energy levels and electromagnetic properties in the truncated NPA space. Similar to the cases of ^{136}Xe and ^{138}Ba, the S, D, G, I_1, and

TABLE III. One-dimensional, optimized nucleon-pair basis states, for which the overlaps with corresponding SM wave functions are larger than 0.85, and the dimensions of corresponding SM and NPA configuration spaces, for the ^{136}Xe nucleus. S,P,D,F,G,H represent positive-parity nucleon pairs with spin $J = 0,1,2,3,4,5$, respectively, and I_1, I_2 represent the two positive-parity spin-six pairs. $\mathcal{F},\mathcal{G},\mathcal{H},\mathcal{I},\mathcal{J},\mathcal{K},\mathcal{L}$ correspond to negative-parity nucleon pairs with spin $J = 3,4,5,6,7,8,9$, respectively.

J^P	Dimension		Pair state
	SM	NPA	
0_1^+	50	6	$\|S^2\rangle$
1_1^+	90	2	$\|SP\rangle$
2_1^+	166	9	$\|SD\rangle$
3_1^+	166	5	$\|SF\rangle$
4_1^+	197	11	$\|SG\rangle$
5_1^+	165	7	$\|SH\rangle$
6_1^+	161	11	$\|SI_1\rangle$
6_2^+	161	11	$\|SI_2\rangle$
8_1^+	114	8	$\|DI_2\rangle$
8_2^+	114	8	$\|DI_1\rangle$
9_1^+	80	3	$\|I_1I_2\rangle$
10_1^+	71	5	$\|GI_2\rangle$
			$\|I_1I_1\rangle$
3_1^-	130	7	$\|S\mathcal{F}\rangle$
4_1^-	160	7	$\|S\mathcal{G}\rangle$
5_1^-	175	8	$\|S\mathcal{H}\rangle$
6_1^-	175	7	$\|S\mathcal{I}\rangle$
7_1^-	162	8	$\|S\mathcal{J}\rangle$
8_1^-	135	7	$\|S\mathcal{K}\rangle$
9_1^-	103	7	$\|S\mathcal{L}\rangle$
11_1^-	47	4	$\|D\mathcal{L}\rangle$
13_1^-	16	3	$\|I_1\mathcal{L}\rangle$
14_1^-	8	2	$\|I_1\mathcal{L}\rangle$
			$\|I_2\mathcal{L}\rangle$

I_2 pairs with positive parity and even spin are adopted to construct positive-parity configuration space. As shown in Tables III and IV, the negative-parity yrast states of ^{136}Xe and ^{138}Ba, with spin $J = 3,4,5,6,7,8,9$, are well described to be seniority-two states, and the negative-parity yrast states with spin $J > 9$ are well represented by the optimized pair basis state constructed by coupling the $\mathcal{L}$ (negative-parity and spin-nine) pair to the above positive-parity pairs. For ^{140}Ce and ^{142}Nd, the negative-parity configuration space is constructed by coupling the $\mathcal{L}$ pair to the positive-parity pairs, and the seniority-two pair basis states $|S^{(N-1)}J^P\rangle$ with $J^P = 3^-,4^-,5^-,6^-,7^-,8^-$ are additionally included. As the yrast states with $J^P = 1^+,3^+,5^+$ are also expected to be seniority-two states, corresponding seniority-two pair basis states are also included in our calculations.

To reduce the dimension of the NPA space for ^{140}Ce and ^{142}Nd, the maximum number of the non-S pairs in each pair basis is limited to be three for ^{140}Ce and two for ^{142}Nd. As valence protons still predominantly occupy the $g_{7/2}$ and $d_{5/2}$ orbits in the low-lying positive-parity states of these two nuclei, and we consider at most six unpaired nucleons (not coupled to S pairs) for ^{140}Ce and at most four for ^{142}Nd, we discuss low-lying positive-parity states with spin up to 12 for ^{140}Ce and

TABLE IV. Same as in Table III except for the ^{138}Ba nucleus. For the pair basis state with three non-S pairs, we denote $((A^{r_1\dagger} \times A^{r_2\dagger})^{(J_2)} \times A^{r_3\dagger})^{(J_3)}|0\rangle$ by using $|r_1r_2r_3,J_2\rangle$ without confusion. J_3 is suppressed, and J_2 is also suppressed in the case of $r_1 = 0$.

J^P	Dimension		Pair state
	SM	NPA	
0_1^+	518	24	$\|S^3\rangle$
1_1^+	1281	22	$\|S^2P\rangle$
2_1^+	2134	60	$\|S^2D\rangle$
3_1^+	2602	57	$\|S^2F\rangle$
4_1^+	3053	86	$\|S^2G\rangle$
5_1^+	3110	71	$\|S^2H\rangle$
6_1^+	3170	93	$\|S^2I_1\rangle$
6_2^+	3170	93	$\|S^2I_2\rangle$
8_1^+	2715	71	$\|SDI_1\rangle$
8_2^+	2715	71	$\|SDI_2\rangle$
9_1^+	2320	56	$\|SI_1I_2\rangle$
10_1^+	2000	56	$\|SI_2I_2\rangle$
11_1^+	1576	34	$\|I_1I_1I_2,8\rangle$
			$\|I_1I_1I_2,10\rangle$
			$\|I_1I_2I_2,5\rangle$
			$\|I_1I_2I_2,7\rangle$
12_1^+	1255	33	$\|GI_1I_2,8\rangle$
3_1^-	2455	83	$\|S^2\mathcal{F}\rangle$
4_1^-	2896	89	$\|S^2\mathcal{G}\rangle$
5_1^-	3151	107	$\|S^2\mathcal{H}\rangle$
6_1^-	3221	105	$\|S^2\mathcal{I}\rangle$
7_1^-	3098	115	$\|S^2\mathcal{J}\rangle$
8_1^-	2821	104	$\|S^2\mathcal{K}\rangle$
9_1^-	2444	103	$\|S^2\mathcal{L}\rangle$
11_1^-	1577	76	$\|SD\mathcal{L}\rangle$
13_1^-	853	50	$\|SI_1\mathcal{L}\rangle$
14_1^-	584	35	$\|SI_1\mathcal{L}\rangle$
			$\|SI_2\mathcal{L}\rangle$
15_1^-	389	29	$\|GI_2\mathcal{L},7\rangle$
16_1^-	243	17	$\|I_1I_2\mathcal{L},7\rangle$
17_1^-	145	12	$\|GI_1\mathcal{L},10\rangle$
			$\|I_1I_2\mathcal{L},10\rangle$

TABLE V. Overlaps between the NPA wave functions of negative-parity yrast states with spin J and the one-octupole-phonon excited states obtained by coupling the octupole operator Q^3 to the NPA wave functions of corresponding positive-parity states with spin J', $J - J' = 3$.

J^-	J'^+	overlap	
		^{136}Xe	^{138}Ba
9_1^-	6_1^+	0.78	0.84
9_1^-	6_2^+	0.92	0.75
10_1^-	7_1^+	0.90	0.84
11_1^-	8_1^+	0.89	0.87
11_1^-	8_2^+	0.78	0.03
12_1^-	9_1^+	0.95	0.89
13_1^-	10_1^+	0.84	0.34
14_1^-	11_1^+	–	0.04
15_1^-	12_1^+	–	0.97

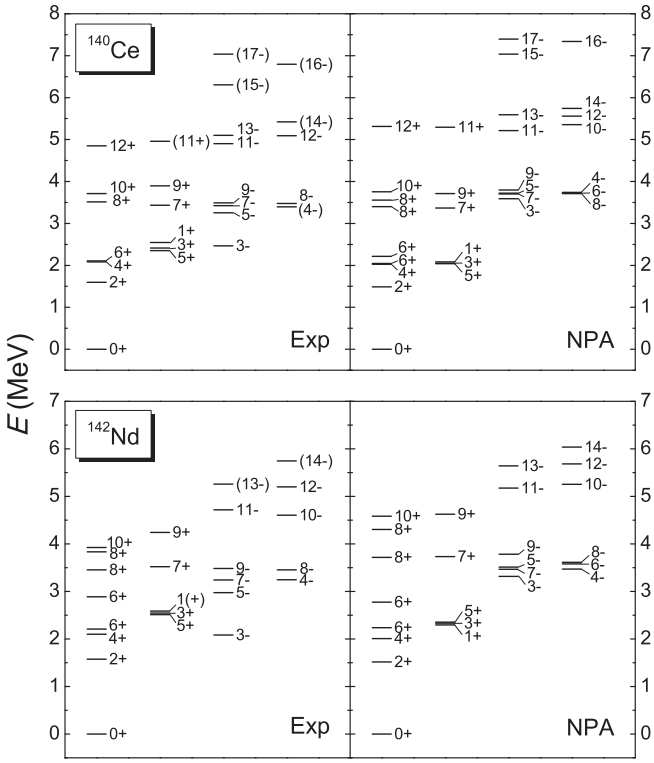

FIG. 4. Energy levels of ^{140}Ce and ^{142}Nd calculated in the truncated NPA spaces, in comparison with experimental data from Refs. [12,33].

10 for ^{142}Nd. Similarly, we discuss low-lying negative-parity states with spin up to 17 for ^{140}Ce and 14 for ^{142}Nd.

In Fig. 4 we present the calculated energy levels of ^{140}Ce and ^{142}Nd obtained in the above truncated NPA spaces, in comparison with experimental data. In Fig. 4 one sees the experimental energy levels of these two nuclei are well reproduced in our calculations, except for the 10^-_1 and 12^-_1 states of ^{142}Nd. The deviation of these two states might be originated from the absence of some relevant pair configurations in the NPA spaces. In Table VI we present calculated $B(E2)$, $B(E3)$, μ values of ^{140}Ce and ^{142}Nd, and corresponding experimental data. The effective charges and gyromagnetic ratios are set the same as those adopted for ^{134}Te, ^{136}Xe, and ^{138}Ba. One sees that experimental data are reasonably reproduced in our calculations.

It is worthwhile to investigate for ^{140}Ce and ^{142}Nd whether the NPA wave function of each low-lying state discussed here can be represented by the one-dimensional nucleon-pair basis state. For ^{140}Ce, the NPA wave functions of the yrast positive-parity states with spin up to 12 and negative-parity states with spin up to 17, as well as the 6^+_2 and 8^+_2 states, can be well represented by the optimized pair basis states (the corresponding overlaps are larger than 0.89), except for the 12^-_1 state. For ^{142}Nd, the NPA wave functions of the yrast positive-parity states with spin up to 10 and negative-parity states with spin up to 14, as well as the 6^+_2 and 8^+_2 states, can also be well represented by the optimized pair basis states.

TABLE VI. Calculated $B(E2)$ and $B(E3)$ values (in units of W.u.), and magnetic moments μ (in units of μ_N) of ^{140}Ce and ^{142}Nd, in comparison with experimental data [33]. The effective charges and gyromagnetic ratios are set the same as those adopted for ^{134}Te, ^{136}Xe, and ^{138}Ba.

	^{140}Ce		^{142}Nd	
	Exp	NPA	Exp	NPA
$B(E2)$				
$2^+_1 \to 0^+_1$	13.8(3)	14.02	12.03(22)	13.53
$4^+_1 \to 2^+_1$	0.137(4)	1.18	–	0.51
$6^+_1 \to 4^+_1$	0.29(6)	0.05	–	0.05
$6^+_2 \to 4^+_1$	–	0.25	–	<0.01
$8^+_1 \to 6^+_1$	–	0.59	–	4.28
$8^+_1 \to 6^+_2$	–	5.28	–	<0.01
$8^+_2 \to 6^+_1$	–	5.54	–	0.07
$8^+_2 \to 6^+_2$	–	0.39	–	7.66
$10^+_1 \to 8^+_1$	0.46(13)	3.03	–	0.09
$10^+_1 \to 8^+_2$	–	0.24	–	0.20
$12^+_1 \to 10^+_1$	–	0.29	–	–
$5^-_1 \to 3^-_1$	–	<0.01	–	0.67
$7^-_1 \to 5^-_1$	–	0.07	–	0.51
$9^-_1 \to 7^-_1$	–	<0.01	–	0.03
$11^-_1 \to 9^-_1$	–	9.23	–	10.64
$13^-_1 \to 11^-_1$	–	<0.01	–	0.23
$15^-_1 \to 13^-_1$	–	0.57	–	–
$17^-_1 \to 15^-_1$	–	1.25	–	–
$B(E3)$				
$9^-_1 \to 6^+_1$	–	9.94	–	8.21
$9^-_1 \to 6^+_2$	–	0.06	–	0.02
$11^-_1 \to 8^+_1$	–	0.30	–	7.11
$11^-_1 \to 8^+_2$	–	7.92	–	0.24
$13^-_1 \to 10^+_1$	–	14.31	–	0.51
$15^-_1 \to 12^+_1$	–	11.71	–	–
μ				
2^+_1	1.9(2)	2.30	1.69(15)	2.74
4^+_1	4.35(10)	4.26	–	6.53
6^+_1	–	6.83	–	6.89
6^+_2	–	4.84	–	4.75
8^+_1	–	7.97	–	10.01
8^+_2	–	9.18	–	7.65
10^+_1	10.3(4)	11.33	7.9(24)	11.33
12^+_1	–	13.18	–	–

According to our NPA wave functions, the 0^+_1 states of ^{140}Ce and ^{142}Nd are represented by the collective-S-pair condensation; the yrast positive-parity states with spin $J = 1,2,3,4,5,6$ and negative-parity states with $J = 3,4,5,6,7,8,9$, as well as the 6^+_2 state, are well described to be seniority-two states, which means they can be represented by the pair basis states in the form of $|S^{(N-1)}J^P\rangle$. The positive-parity yrast states with $J > 6$, as well as the 8^+_2 state, are represented by the optimized pair basis states having two or three non-S pairs, at least one of which is the I_1 or I_2 pair; the negative-parity yrast states with $J > 9$ are represented by the pair basis states also having two or three non-S pairs, one of which is the $\mathcal{L}$ pair. In other words, for these two nuclei, the low-lying positive-parity yrast states with $J > 6$ are given by breaking S pair(s) of the

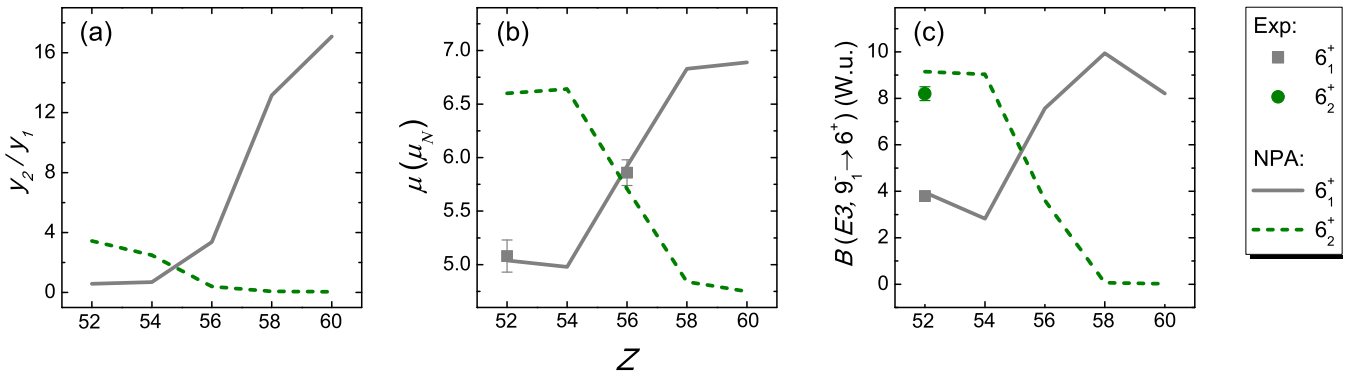

FIG. 5. (a) Ratio between the two structure coefficients $y(g_{7/2}d_{5/2}6)$ and $y(g_{7/2}g_{7/2}6)$ (denoted as y_2/y_1) for the I_1 and I_2 pairs, versus proton number Z. (b) $\mu(6_1^+)$ and $\mu(6_2^+)$ values versus Z. (c) $B(E3)$ values of the two transitions $9_1^- \rightarrow 6_1^+$ and $9_1^- \rightarrow 6_2^+$, versus Z. Experimental data are taken from Ref. [33].

6_1^+ or 6_2^+ state, and the negative-parity yrast states with $J > 9$ are given by breaking S pair(s) of the 9_1^- state, similar to the cases of ^{136}Xe and ^{138}Ba.

C. Evolution of the 6_1^+ and 6_2^+ states

It is interesting to study the evolution of the 6_1^+ and 6_2^+ states for the five isotones. As the 6_1^+ and 6_2^+ states for the five isotones are represented by the pair basis states constructed by coupling $(N-1)$ S pairs to the I_1 and I_2 pairs, respectively, the structure coefficients of the I_1 and I_2 pairs are very important to the properties of these two states, such as magnetic moments. As the 9_1^- state of the five isotones is well represented by coupling $(N-1)$ S pairs to the $\mathcal{L}$ pair which is defined uniquely by $(g_{7/2} \otimes h_{11/2})_{9^-}$, the structure coefficients of the I_1 and I_2 pairs are crucial to the $B(E3)$ values of the transitions $9_1^- \rightarrow 6_1^+$ and $9_1^- \rightarrow 6_2^+$, respectively.

As the $(h_{11/2} \otimes h_{11/2})_{6^+}$ configuration is negligible in both the I_1 and I_2 pairs, the ratio between the pair structure coefficient of $(g_{7/2} \otimes d_{5/2})_{6^+}$ (denoted by y_2) and that of $(g_{7/2} \otimes g_{7/2})_{6^+}$ (denoted by y_1) defines the I_1 and I_2 pairs. In Fig. 5 we present the y_2/y_1 values of the I_1 and I_2 pairs, the magnetic moments of the 6_1^+ and 6_2^+ states, and the $B(E3)$ values of the transitions $9_1^- \rightarrow 6_1^+$ and $9_1^- \rightarrow 6_2^+$, respectively, versus proton number Z. In Fig. 5(a) one sees, for the I_1 pair, y_2/y_1 increases with proton number; and for the I_2 pair, the value of y_2/y_1 behaves in an opposite way. For the magnetic moments, as the g factor of one proton in the $g_{7/2}$ orbit is considerably smaller than that of one proton in the $d_{5/2}$ orbit, the $(g_{7/2} \otimes g_{7/2})_{6^+}$ component gives a smaller magnetic moment than the $(g_{7/2} \otimes d_{5/2})_{6^+}$ component. One therefore expects the $\mu(6_1^+)$ value increases with proton number while the $\mu(6_2^+)$ value decreases, and this is indeed the case of experimental data for the 6_1^+ state shown in Fig. 5(b). For the $B(E3)$ values, the spin-flip single particle transformation $h_{11/2} \rightarrow g_{7/2}$ gives rise to the retarded $E3$ transition, in comparison with the transformation $h_{11/2} \rightarrow d_{5/2}$ [24]. One then expects that the $B(E3, 9_1^- \rightarrow 6_1^+)$ value increases with proton number (despite small decreases for ^{136}Xe and ^{142}Nd), while the $B(E3, 9_1^- \rightarrow 6_2^+)$ value decreases. Experimental measurements of these magnetic moments and $B(E3)$ values are warranted in the future.

IV. SUMMARY

In this paper we study energy levels and electromagnetic properties of the $N = 82$ isotones ^{134}Te, ^{136}Xe, ^{138}Ba, ^{140}Ce, and ^{142}Nd, within the nucleon-pair approximation (NPA). Our NPA calculations reproduce well experimental data of energy levels, $B(E2)$, $B(E3)$ and magnetic moments. We also tabulate our predicted transition rates and magnetic moments of low-lying states for these nuclei.

For ^{136}Xe and ^{138}Ba, the calculation is performed in the full SM space, the truncated NPA space, and the one-dimensional spaces constructed by the optimized pair basis states, respectively. It is shown that, for the low-lying yrast states with positive or negative parity, as well as the 6_2^+ and 8_2^+ states, the overlap between the SM wave function and the NPA wave function is very close to 1, with few exceptions. It is also very interesting to note that most SM wave functions of these states, including those with seniority four and six, are well approximated by one-dimensional, optimized nucleon-pair basis states. Therefore we call them "pair states" to highlight this simplicity.

For ^{136}Xe and ^{138}Ba, based on the optimized pair basis states, the low-lying positive-parity yrast states with spin $J > 6$, as well as the 8_2^+ state, are approximately given by breaking one or two S pair(s) of the 6_1^+ or 6_2^+ state (the low-lying, seniority-two, spin-maximum, and positive-parity states), which means that these positive-parity states can be approximately regarded as excited states of the 6_1^+ or 6_2^+ state. Similarly, the low-lying negative-parity yrast states with spin $J > 9$ are well described by breaking one or two S pair(s) of the 9_1^- state, which means that these negative-parity states can be approximately taken to be excited states with respect to the 9_1^- state.

Our calculation also suggests the negative-parity yrast states with $J = 9 \sim 13$ for ^{136}Xe and with $J = 9 \sim 15$ for ^{138}Ba can be explained as one-octupole-phonon states, with few exceptions. Interestingly, it is shown that the 9_1^- state of ^{136}Xe is better represented by coupling the octupole phonon to the 6_2^+ state rather than to the 6_1^+ state, while the 9_1^- state of

^{138}Ba is better represented by coupling the octupole phonon to the 6_1^+ state, which is consistent with the suggestion of Ref. [25].

For most low-lying yrast states of ^{140}Ce and ^{142}Nd, as well as the 6_2^+ and 8_2^+ states, the NPA wave functions can be well represented by the one-dimensional, optimized pair basis states. Based on the optimized pair basis states, the features for these two nuclei are similar to those for ^{136}Xe and ^{138}Ba.

The 6_1^+ and 6_2^+ states of these five isotones are also investigated systematically. They are well represented by the pair basis states constructed by coupling $(N-1)$ S pairs to the I_1 and I_2 pairs, respectively. If the very small component of two protons in the $h_{11/2}$ orbit is neglected, the ratio of pair structure coefficients, $y(g_{7/2}d_{5/2}6)/y(g_{7/2}d_{7/2}6)$, defines the structure of the I_1 and I_2 pairs. This ratio increases with proton number for the I_1 pair, and decreases for the I_2 pair. Such an evolution of $y(g_{7/2}d_{5/2}6)/y(g_{7/2}d_{7/2}6)$ leads to a pattern of magnetic moments and $B(E3)$ transition rates versus proton number, as shown in Fig. 5.

In this work we adopt the phenomenological Hamiltonian, which gives a satisfactory description of both energy levels and electromagnetic properties. The simple picture of pair states will be further investigated by using realistic interactions.

ACKNOWLEDGMENTS

We thank the National Natural Science Foundation of China (Grants No. 11225524 and No. 11505113), the 973 Program of China (Grant No. 2013CB834401), Shanghai Key Laboratory of Particle Physics and Cosmology (Grant No. 11DZ2260700), the Program of Shanghai Academic/Technology Research Leader (Grant No. 16XD1401600), and China Postdoctoral Science Foundation (Grant No. 2015M580319) for financial support. This work is also supported by the Center for High Performance Computing (HPC) at Shanghai Jiao Tong University.

[1] A. Holt, T. Engeland, E. Osnes, M. Hjorth-Jensen, and J. Suhonen, Nucl. Phys. A **618**, 107 (1997).
[2] L. Coraggio, A. Covello, A. Gargano, N. Itaco, and T. T. S. Kuo, Phys. Rev. C **80**, 044320 (2009).
[3] A. Ansari and P. Ring, Phys. Lett. B **649**, 128 (2007).
[4] B. H. Wildenthalt, Phys. Rev. Lett. **22**, 1118 (1969).
[5] B. H. Wildenthal and D. Larson, Phys. Lett. **37**, 266 (1971).
[6] J. Sau, K. Heyde, and R. Chéry, Phys. Rev. C **21**, 405 (1980).
[7] Z. Berant, A. Wolf, J. C. Hill, F. K. Wohn, R. L. Gill, H. Mach, M. Rafailovich, H. Kruse, B. H. Wildenthal, G. Peaslee, A. Aprahamian, J. Goulden, and C. Chung, Phys. Rev. C **31**, 570 (1985).
[8] F. Andreozzi, L. Coraggio, A. Covello, A. Gargano, T. T. S. Kuo, and A. Porrino, Phys. Rev. C **56**, R16 (1997).
[9] P. J. Daly, P. Bhattacharyya, C. T. Zhang, Z. W. Grabowski, R. Broda, B. Fornal, I. Ahmad, T. Lauritsen, L. R. Morss, W. Urban, W. R. Phillips, J. L. Durell, M. J. Leddy, A. G. Smith, B. J. Varley, N. Schulz, E. Lubkiewicz, M. Bentaleb, and J. Bomqvist, Phys. Rev. C **59**, 3066 (1999).
[10] S. Sarkar and M. S. Sarkar, Phys. Rev. C **64**, 014312 (2001).
[11] B. A. Brown, N. J. Stone, J. R. Stone, I. S. Towner, and M. Hjorth-Jensen, Phys. Rev. C **71**, 044317 (2005).
[12] A. Astier, M.-G. Porquet, Ts. Venkova, D. Verney, Ch. Theisen, G. Duchêne, F. Azaiez, G. Barreau, D. Curien, I. Deloncle, O. Dorvaux, B. J. P. Gall, M. Houry, R. Lucas, N. Redon, M. Rousseau, and O. Stézowski, Phys. Rev. C **85**, 064316 (2012).
[13] D. Bianco, N. Lo Iudice, F. Andreozzi, A. Porrino, and F. Knapp, Phys. Rev. C **88**, 024303 (2013).
[14] I. Talmi, Nucl. Phys. A **172**, 1 (1971).
[15] S. Shlomo and I. Talmi, Nucl. Phys. A **198**, 81 (1972).
[16] I. Talmi, *Simple Models of Complex Nuclei* (Harwood Academic, Chur, Switzerland, 1993).
[17] Y. K. Gambhir, A. Rimini, and T. Weber, Phys. Rev. **188**, 1573 (1969).
[18] K. Allart, E. Boeker, G. Bonsignori, M. Saroia, and Y. K. Gambhir, Phys. Rep. **169**, 209 (1988).
[19] O. Scholten and H. Kruse, Phys. Lett. B **125**, 113 (1983).
[20] N. Sandulescu, J. Blomqvist, T. Engeland, M. Hjorth-Jensen, A. Holt, R. J. Liotta, and E. Osnes, Phys. Rev. C **55**, 2708 (1997).
[21] D. J. Dean and M. Hjorth-Jensen, Rev. Mod. Phys. **75**, 607 (2003).
[22] M. P. Kartamyshev, T. Engeland, M. Hjorth-Jensen, and E. Osnes, Phys. Rev. C **76**, 024313 (2007).
[23] M. A. Caprio, F. Q. Luo, K. Cai, V. Hellemans, and Ch. Constantinou, Phys. Rev. C **85**, 034324 (2012).
[24] J. P. Omtvedt, H. Mach, B. Fogelberg, D. Jerrestam, M. Hellström, L. Spanier, K. I. Erokhina, and V. I. Isakov, Phys. Rev. Lett. **75**, 3090 (1995).
[25] J. K. Hwang, J. H. Hamilton, and A. V. Ramayya, Eur. Phys. J. A **49**, 125 (2013).
[26] J. K. Hwang, J. H. Hamilton, A. V. Ramayya, and Y. X. Luo, J. Phys. G: Nucl. Part. Phys. **40**, 065106 (2013).
[27] J. Q. Chen, Nucl. Phys. A **626**, 686 (1997).
[28] Y. M. Zhao, N. Yoshinaga, S. Yamaji, J. Q. Chen, and A. Arima, Phys. Rev. C **62**, 014304 (2000).
[29] G. J. Fu, Y. Lei, Y. M. Zhao, S. Pittel, and A. Arima, Phys. Rev. C **87**, 044310 (2013).
[30] Y. Lei, Z. Y. Xu, Y. M. Zhao, and A. Arima, Phys. Rev. C **80**, 064316 (2009); **82**, 034303 (2010).
[31] H. Jiang, Y. Lei, G. J. Fu, Y. M. Zhao, and A. Arima, Phys. Rev. C **86**, 054304 (2012); H. Jiang, Y. Lei, C. Qi, R. Liotta, R. Wyss, and Y. M. Zhao, *ibid.* **89**, 014320 (2014).
[32] Y. M. Zhao and A. Arima, Phys. Rep. **545**, 1 (2014), and references therein.
[33] http://www.nndc.bnl.gov/ensdf/.
[34] Y. M. Zhao, S. Yamaji, N. Yoshinaga, and A. Arima, Phys. Rev. C **62**, 014315 (2000).